

The real time evolution of post-AGB stars

Marcin Hajduk 

University of Warmia and Mazury, ul. Oczapowskiego 2, 10-719 Olsztyn, Poland,
email: marcin.hajduk@uwm.edu.pl

Abstract. Evolution of post-AGB stars is extremely fast. They cross the HR diagram vertically on a timescale of hundreds to some ten thousands of years to reach maximum temperature in their lifetime. This is reflected in an increasing excitation of planetary nebulae on a timescale of years and decades. Since evolutionary timescale of post-AGB stars is very sensitive to their mass, observed changes can be used to determine model dependent central star masses. If an additional parameter is determined (e.g. luminosity or dynamic age), the observed evolution of planetary nebulae can be utilized for observational verification of theoretical models.

Keywords. stars: AGB and post-AGB, planetary nebulae: general, white dwarfs, stars: evolution, stars: fundamental parameters, Hertzsprung-Russell diagram

1. Introduction

Post-AGB stars evolve from the stars with initial masses from 1 to 8 M_{\odot} . The star loses most of its envelope on the tip of the asymptotic giant branch (AGB). Once the star is hot enough, the ionization front expands throughout the ejected shell, creating a planetary nebula (PN). A post-AGB star crosses the HR diagram horizontally on a timescale τ_{cross} ranging from tens to tens thousands of years. After the star reaches maximum temperature in its lifetime (Herwig 2005), it gradually descend on the white dwarf (WD) cooling track.

Only a few sets of evolutionary models had been available till recently, including Bloeker (1995) and Vassiliadis & Wood (1994). The models demonstrate that τ_{cross} depends critically on the central star mass. More massive remnants evolve three or more orders of magnitude faster than the least massive ones. The duration of the post-AGB phase is determined by the remaining mass of the hydrogen envelope after AGB phase. For low mass remnants, the envelope is consumed at the H burning rate. For more massive remnants, mass loss due to the stellar wind can significantly shorten the evolutionary timescale (Bloeker 1995).

Gesicki *et al.* (2014) needed to accelerate the Bloeker's post-AGB tracks by a factor of three, so that central stars, derived from stellar-mass - age relation, could match the local WD masses. New models by Miller-Bertolami (2016) confirmed their results and predicted 3 to 10 times faster evolution than the previous authors. Models computed by Miller-Bertolami (2016) leave AGB with significantly reduced H envelope mass compared to previous models. This difference was attributed to an updated treatment of the constitutive microphysics and updated description of the mixing processes and winds. Post-AGB timescales only show a mild dependence on metallicity in Miller-Bertolami (2016), contrary to the previous authors.

2. Observational verification of evolutionary models

The crossing time τ_{cross} calculated in post-AGB models depends critically on the central star mass. τ_{cross} is too long to be observed. Instead, we can use heating rate \dot{T}_{eff} .

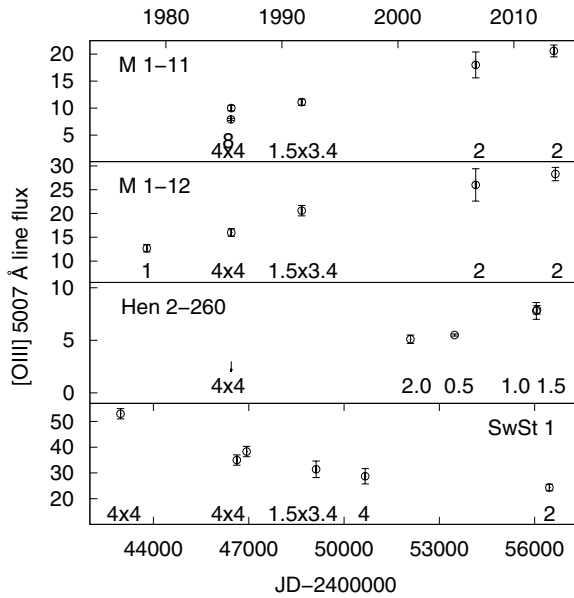


Figure 1. Temporal evolution of the [O III] 5007Å / Hβ flux ratio in selected PNe observed at more than two epochs. The numbers indicate aperture widths used in each observation.

Hajduk *et al.* (2015) showed that \dot{T}_{eff} does not change significantly throughout the horizontal part of the evolution. Post-AGB stars evolve at constant luminosity till they reach T_{eff} of 10^4 K or more. Luminosity is also sensitive to the mass of post-AGB star. Both \dot{T}_{eff} and L_* have to be determined for the same star to verify evolutionary models. If evolutionary model is correct, both \dot{T}_{eff} and L_* should indicate the same mass of the post-AGB star.

Heating rate can be derived from observations of the central star or/and the nebula covering a time span of several years by means of atmosphere or/and photoionization modeling. Temperature evolution was measured for a few stars experiencing late or very late thermal pulse: FG Sge (Jeffery & Schönberner 2006), V605 Aql Clayton (2006), V4334 Sgr (van Hoof *et al.* 2007), and recently SAO 244567 (Reindl *et al.* 2017), which largely contributed to our understanding of this special case of post-AGB evolution.

In this paper we focus on the study of post-AGB stars which are not known to experience late thermal pulses. We included hydrogen deficient post-AGB central stars, which evolutionary status is not yet fully understood. Although their evolution is slower, \dot{T}_{eff} was also determined for a few central stars which are not known to have experienced (late) thermal pulse. Hydrogen deficient stars are hydrogen burners, while hydrogen rich post-AGB stars can be either helium or hydrogen burners. Evolution of helium burning post-AGB stars proceeds slower than that of hydrogen burning stars.

Zijlstra *et al.* (2008) determined \dot{T}_{eff} of $156 \pm 36 \text{ K yr}^{-1}$ for the central star of NGC 7027, and Hajduk *et al.* (2014) $45 \pm 7 \text{ K yr}^{-1}$ for the central star of Hen 2-260. The nebular variability was reported in IC 4997 and NGC 6572 by Feibelman *et al.* (1992) and in M 1-11 and M 1-6 by Kondratyeva (2005) without giving the heating rates. Hajduk *et al.* (2015) observed increase of the excitation of many young planetary nebulae on a timescale of years and decades (Fig. 1). Unexpectedly, the central star of the PN SwSt 1 showed decreasing temperature, inconsistent with evolutionary models (Hajduk *et al.*, in prep.).

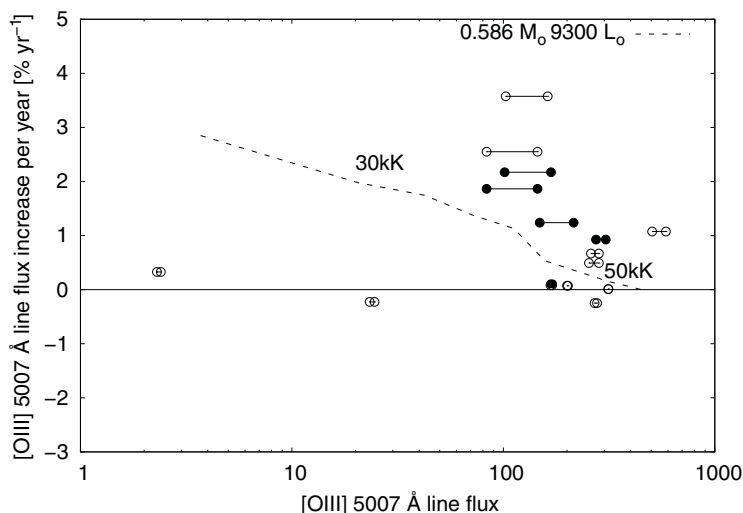


Figure 2. Temporal evolution of the $[\text{O III}] 5007\text{\AA} / H\beta$ flux ratio in Magellanic Clouds PNe. The dashed lines plot the evolutionary tracks by Miller-Bertolami (2016). Filled symbols show post-AGB stars which show emission lines in their spectra.

3. New observations and preliminary results

We observed a new sample of young southern PNe with the New Technology Telescope and South African Large Telescope. We focused on low excitation $F([\text{O III}] 5007\text{\AA}) / F(H\beta) < 5$ and compact ($d < 5$ arc sec) PNe. Small observed diameters of the PNe allow to avoid systemic errors related with the ion stratification within the nebula, as the slit width probes most of or all the nebular light. Each PN was previously observed at least one time, most of them by Acker *et al.* (1992). Unfortunately, only six of the Galactic PNe in the sample have a precise distance determination with GAIA better than 30% (Kimeswenger & Barria 2018) (the observations were performed before the launch of GAIA mission). Accurate determination of the luminosities is necessary for verification of the evolutionary tracks. Some 20 SMC and LMC PNe were observed as well. These objects can be used for the verification of evolutionary tracks as their distances and luminosities are known.

Fig. 2 shows clear evidence for evolution of the $[\text{O III}] 5007\text{\AA} / H\beta$ flux ratio for some of the Magellanic Cloud PNe. Interestingly, the evolution is significantly faster than predicted for the $0.586M_{\odot}$ evolutionary track. Two coolest post-AGB stars do not show evidence for flux evolution, which may indicate that they are very low mass stars.

We obtained a model using photoionization code CLOUDY (Ferland *et al.* 2017) for two of the observed PNe so far. The measured line fluxes and other data available in the literature served as input parameters. In this preliminary work we used reference spectra, abundances, and luminosities provided by Leisy & Dennefeld (2006) and Dopita & Meatheringham (1991).

Initially, we found the best solution for temperature for one epoch. Then we varied the central star temperature to fit optical line fluxes observed in other epoch. Luminosity remains constant for young PNe, so the changing nebular flux ratios reflect the evolution of stellar temperature and to much smaller extent expansion. As a result, we derived the difference of the stellar temperature between the two epochs. It is illustrated in Fig. 3. The determined \dot{T}_{eff} for LHA 120 N199 of 30 K yr^{-1} , and for SMP SMC 1 even higher – of 130 K yr^{-1} . They exceed the expected heating rates expected from their luminosities.

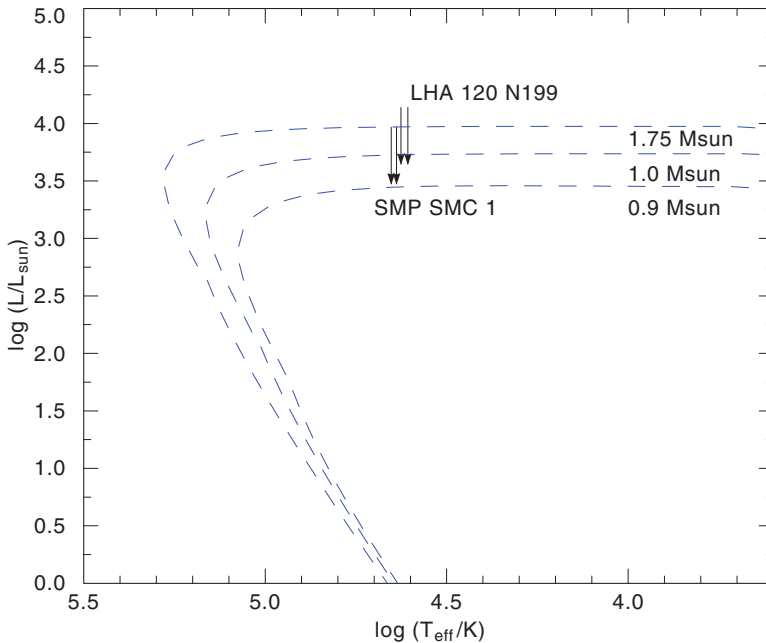


Figure 3. Temporal evolution of two central stars of PNe in Magellanic Clouds in the HR diagram. Two arrows for each object correspond to two different epochs. The dashed lines plot the evolutionary tracks by Miller-Bertolami (2016).

Acknowledgments

We gratefully acknowledge financial support from National Science Centre, Poland, grant No. 2016/23/B/ST9/01653. Some of the observations reported in this paper were obtained with the Southern African Large Telescope (SALT). Polish participation in SALT is funded by grant No. MNiSW DIR/WK/2016/07. Based on observations collected at the European Organisation for Astronomical Research in the Southern Hemisphere under ESO programmes 093.D-0182 and 095.D-0614.

References

- Acker, A. *et al.* 1992, *The Strasbourg-ESO Catalogue of Galactic Planetary Nebulae*
 Bloeker, T. 1999, *A&A*, 299, 755
 Clayton, G. 2006, *ApJ*, 646L, 69
 Dopita, M. A. & Meatheringham, S. J. 2006, *ApJ*, 377, 480
 Feibelman, W. A. *et al.* 1992, *PASP*, 104, 339
 Ferland, G. *et al.* 2017, *RMxAA*, 53, 385
 Gesicki, K., Zijlstra, A. A., Hajduk, M., & Szyszka, C. 2014, *A&A*, 566A, 48
 Hajduk, M. *et al.* 2014, *A&A*, 567A, 15
 Hajduk, M., van Hoof, P. A. M., & Zijlstra, A. A. 2015, *A&A*, 573A, 65
 Herwig, F. 2005, *ARA&A*, 43, 435
 Jeffery, C. S. & Schönberner, D. 2006, *A&A*, 459, 885
 Kimeswenger, S. & Barria, D. 2018, *A&A*, 616L, 2
 Kondratyeva, L. N. 2005, *Astronomical and Astrophysical Transactions*, 24, 291
 Leisy, P. & Dennefeld, M. 2006, *A&A*, 456, 451
 Miller-Bertolami, M. M. 2016, *A&A*, 588A, 25
 Reindl, N. *et al.* 2017, *MNRAS*, 464, 51
 Vassiliadis, E. & Wood, P. R. 1994, *ApJS*, 92, 125
 van Hoof, P. A. M. *et al.* 2007, *A&A*, 471L, 9
 Zijlstra, A. A. *et al.* 2008, *ApJ*, 681, 1296